Excitons bound at interacting acceptors in $Al_xGa_{1-x}As$/GaAs quantum wells

A. C. Ferreira, P. O. Holtz, and B. Monemar

Department of Physics and Measurements Technology, Linköping University, S-581 83 Linköping, Sweden

M. Sundaram, K. Campman, J. L. Merz, and A. C. Gossard

Center for Quantized Electronic Structures (QUEST), University of California at Santa Barbara, Santa Barbara, California 93016

(Received 14 August 1996)

We have studied the effect of increasing acceptor concentration (between 10^{16} and 10^{18} cm^{-3}) on bound excitons (BE's) using steady-state photoluminescence (PL) and PL excitation spectroscopy. With increasing doping concentration, an additional peak is observed on the low-energy side of the principal neutral acceptor BE. This peak is associated with BE's formed by excitons bound at interacting acceptors, similar to the undulation spectra observed at high acceptor doping in different bulk materials, such as ZnTe, InP, and GaP. The exciton-impurity complexes are formed as the average distance between the acceptor impurities decreases with increasing doping concentration. The dependence of the optical properties of this exciton on temperature, excitation intensity, and magnetic field is presented. [S0163-1829(96)07348-1]

I. INTRODUCTION

The so-called undulation spectrum, a broadband in the excitonic energy range with a regular periodic undulation, attracted great interest in the beginning of the 1970s. Such a peculiar undulation behavior was observed in luminescence spectrum of, e.g., GaP:N containing acceptors.[1] Street and Wiesner[2] showed that the undulatory structure has its origin in the fluctuations of the number of the available impurity pair sites. The undulations were merely the result of averaging the numbers of equivalent sites per N-to-acceptor pair-separation shell.

We studied the effect of various acceptor concentrations on the excitonic states, in particular the acceptor-bound exciton (BE), in quantum wells (QW's) using steady-state photoluminescence (PL) and PL excitation (PLE) measurements. The major recombination channel near the band gap for an undoped GaAs/$Al_xGa_{1-x}As$ QW at low temperatures is the free exciton (FE). For a doped structure, part of the FE's is captured by the available impurities to form BE's. The proportion of BE's relative to the FE's depends mainly on the doping concentration, but also on the well width L_z. The BE recombination channel turns out to be the major process at doping concentrations above 3×10^{16} cm^{-3} for a 150-Å-wide QW.

An increase in the doping concentration corresponds to a decrease in the average distance between the impurities (d_I). If the spatial separation between neighboring acceptors becomes comparable with the extension of the exciton wave function, there will be a further contribution to the potential binding the exciton due to the neighboring acceptor(s). A distribution of binding energies due to the varying spatial separation between the acceptors and possibly also the number of interacting acceptor is expected. There should accordingly be a possibility for excitons to transfer from one site to another site in the neighborhood with a larger binding energy, i.e., at lower transition energy. The interaction between two or more acceptors should increase the binding energy of the exciton compared to an isolated acceptor.

II. EXPERIMENTAL TECHNIQUES

The samples used in this study were grown by molecular beam epitaxy (MBE) at a temperature of nominally 680 °C without interruptions at the QW interfaces. The layers were grown on top of a semi-insulating GaAs (100) substrate with a 0.35-μm undoped GaAs buffer layer. Each structure contains multiple QW structures with 50 periods of alternating layers of GaAs and $Al_xGa_{1-x}As$. The $Al_xGa_{1-x}As$ barriers were 150 Å wide with a nominal Al composition of $x = 0.3$. The wells had a width of 150 Å and were doped with Be in the central 20% of the well at a concentration varying from 10^{16} up to 10^{18} cm^{-3}.

For the PL and PLE measurements, an Ar^+-ion laser was used to pump a tunable titanium-doped sapphire solid-state laser. The emitted light from the samples was focused on the slits of a 1-m double-grating monochromator and detected with a dry-ice-cooled GaAs photomultiplier. The picosecond time-resolved data were obtained at 2 K with excitation from a mode-locked Ar laser and a synchronously pumped dye laser. On the detection side, a synchroscan streak camera in combination with a 0.32-m spectrometer was employed. The time resolution for the combined system is of the order of 10 ps.

Post-growth hydrogen passivation was accomplished at around 190 °C, inside a quartz reactor with a remote dc H plasma at a pressure of 2.0 mTorr. The samples were placed at ~15 cm away from the H discharge region to avoid damage due to ionic impact.

III. RESULTS

Figure 1 displays the development of the PL spectra, measured at low excitation intensity, with increasing acceptor concentration. As can be seen, the excitonic peaks, the acceptor BE, and the heavy-hole (hh) state of the FE are redshifted as the acceptor concentration increases. The observed redshift with increasing acceptor concentration is explained in terms of band-gap renormalization due to the interaction
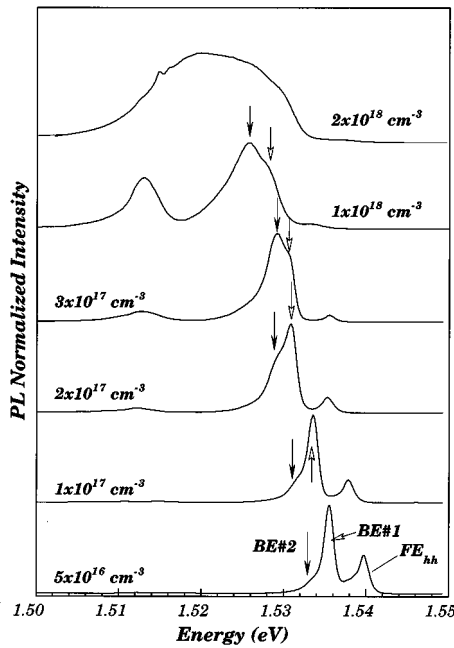
FIG. 1. PL spectra, at low excitation intensity, with increasing doping concentration. The figure shows the development of BE#2 (solid arrows), at the low-energy tail of the principal BE, BE#1 (open arrows). A heavy hole (hh) state of the free exciton (FE) is also indicated.

between the carriers: the exchange-correlation effect.[3] Figure 1 also depicts a peculiar feature on the low-energy side of the principal BE (BE#1). This new component (denoted BE#2 in Fig. 1) visible already at a doping concentration of 5×10^{16} cm^{-3}, gains intensity with increasing doping concentration and becomes dominant at $\approx 3 \times 10^{17}$ cm^{-3}. At high doping concentration ($\geq 2 \times 10^{18}$ cm^{-3}), the double peaks are not resolved owing to broadening effects of the lines. It is noticeable that the double structure for the BE is not observed in PLE (Fig. 2). Instead, the PLE spectrum only reveals the BE#1 blueshifted with respect to PL ($\approx 1 - 3$ meV) accord-
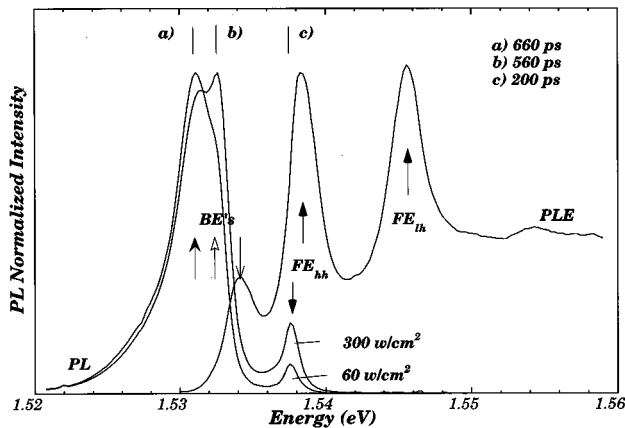

FIG. 2. PL spectra for the sample with an acceptor concentration of 3×10^{17} cm^{-3} for two excitation intensities (300 and 60 W/cm^2). A PLE spectrum is also shown. Arrows indicate excitonic positions and bars [(a), (b), and (c)] the energy position for the decay time measurements.
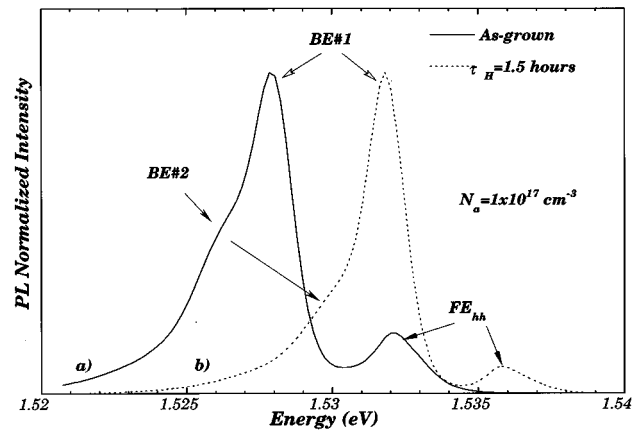

FIG. 3. PL spectra for a sample with doping concentration of 1×10^{17} cm^{-3} (a) ''as grown'' and (b) exposed to 1.5 h hydrogen passivation.

ing to Fig. 2. Such a shift reflects the effect of exciton transfer mechanisms.

It is well known that a hydrogen treatment of bulk samples passivates both shallow dopants and deep centers due to the formation of hydrogen-impurity complexes and a saturation of the dangling bonds.[4] In QW's, hydrogen interacts both with the impurities and interfaces. Accordingly, an increasing passivation level provided by, e.g., a prolonged hydrogenation time (τ_H), has an effect that is similar to an efficient reduction of the acceptor concentration.[5] Figure 3 shows the PL spectrum for a sample with a doping concentration of 1×10^{17} cm^{-3} exposed to hydrogenation during 1.5 h. When compared to an as-grown sample, it is noticeable that the BE#2 component decreases with increasing passivation time. The observed blueshift of the PL spectrum for the passivated sample (b) compared to the ''as-grown'' sample (a) is due to an efficient reduction of the many-body effects and, consequently, an effect opposite to the increase in the doping concentration.[3,5]

The binding energies of both features, BE#1 and BE#2, defined as the energy separation from the FE [plotted in Figs. 4(a) and 4(b)] are found to increase with increasing doping
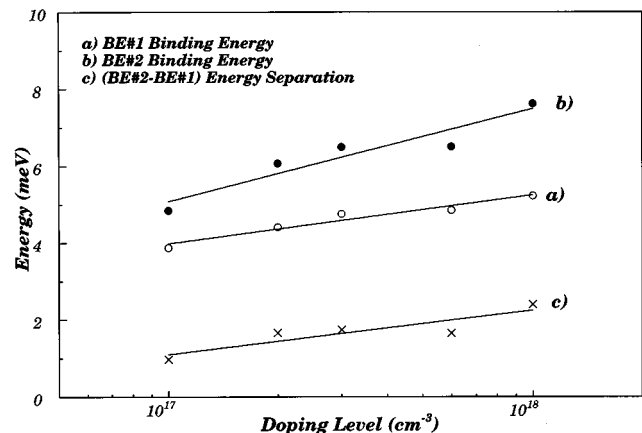

FIG. 4. Dependence of the BE binding energies on the doping concentration [(a), (b)]. The energy separation between BE#1 and BE#2 is shown in (c).
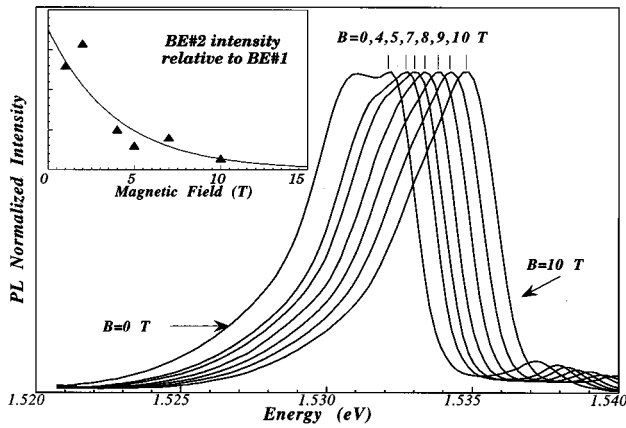
FIG. 5. Magnetic field dependence of the PL spectrum between 0 and 10 T. The inset depicts the intensity of the BE#2 relative to BE#1.
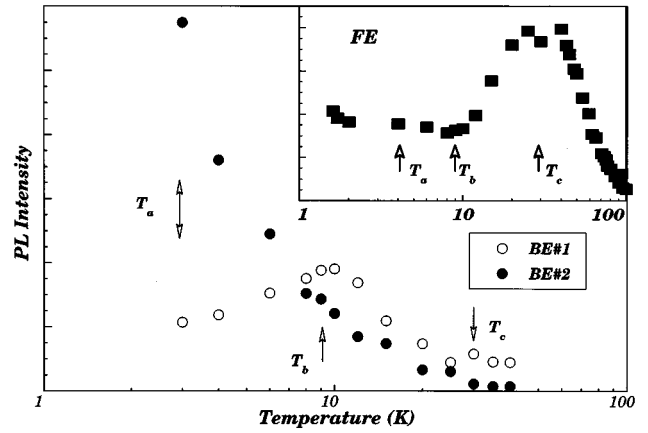

FIG. 6. Temperature dependence of the BE intensity. For clarity we have labeled three ''critical'' temperatures $T_a \approx 3$ K, $T_b \approx 9$ K, and $T_c \approx 60$ K as indicated by opened arrows. In the inset, the FE intensity dependence on the temperature is shown separately.

concentration. The more localized, the BE#2 (with larger binding energy) has a significantly stronger dependence on the doping level. The BE#2 binding energy increases by up to ≈ 3 meV, when the acceptor concentration is increased from 10^{17} up to 10^{18} cm^{-3}, while the BE#1 increases significantly less, by ≈ 1 meV, for the same acceptor concentration increase. Figure 4(c) shows the energy separation between BE#1 and BE#2 plotted against the doping concentration.

The relative intensity of BE#1 versus BE#2 is strongly dependent on the excitation intensity level. This is reflected in the PL spectra shown in Fig. 2 for the sample with an acceptor concentration of 3×10^{17} cm^{-3} for two excitation intensities. Low-intensity levels (below 60 W/cm^2) favor BE#2, while the BE#1 intensity increases continuously with increasing excitation intensity. The PL decay time was measured at 2 K for different detection energies as indicated by bars [(a), (b), and (c)] in Fig. 2. It is found that the decay time is slightly longer for BE#2 [(a) $\tau = 660$ ps] in comparison with BE#1 [(b) $\tau = 560$ ps], while the corresponding decay time for the FE is approximately 200 ps (c).

BE#2 is also sensitive to an applied magnetic field. Figure 5 displays the dependence of the PL spectra on a magnetic field applied parallel to the growth direction of the sample. The energy dependence of the BE#1, BE#2, and FE lines on the applied magnetic field exhibits a quadratic dependence with a diamagnetic shift rate of 2.25×10^{-5}, 2.56×10^{-5}, and 2.80×10^{-5} eV/T^2, respectively. In the inset (Fig. 5) we show the dependence of the BE#2 intensity relative to BE#1. With an applied magnetic field, the intensity of BE#2 decreases relative to BE#1.

Figure 6 shows the temperature dependence of the excitonic intensities. For clarity we have labeled three ''critical'' temperatures $T_a \approx 3$ K, $T_b \approx 9$ K, and $T_c \approx 30$ K as indicated by open arrows. BE#1 has an opposite temperature dependence compared to the FE for $T > T_a$: an increase in intensity up to T_b followed by a reduction. The FE intensity below T_b is approximately constant: After a steep increase, the FE intensity starts to decrease for temperatures above T_c. BE#2, on the other hand, exhibits a steeper decrease, with a quenching at ≈ 45 K, i.e., at a lower temperature than BE#1.

IV. DISCUSSION

BE#1 is associated with the single acceptor BE, i.e., an exciton bound to a neutral isolated acceptor. BE#2, and its low-energy tail, is interpreted as an exciton bound at interacting acceptors. The complex acceptor BE's have similarities with the undulation spectra observed in some bulk materials such as ZnTe,[6–8] InP,[6] and GaP.[1,2,8] We do not observe distinct oscillations in our QW structures as has been the case for well-resolved undulation spectra in bulk materials. However, it should be pointed out that it is possible to observe a few additional peaks at the low-energy side. We analyze below the experimental results described in the former section, based on the properties of three distinct excitonic transitions: the FE, the single acceptor BE (BE#1), and the interacting acceptor BE (BE#2).

In our samples, the dopants are not expected to be homogeneously distributed inside the 30-Å dopant channel in the center of the well. Therefore, it is expected that acceptors at different distances d_I, ranging from distant single noninteracting acceptors to close interacting acceptors, coexist. The increase in the energy separation between BE#1 and BE#2 [Fig. 4(c)] implies that the interaction between the acceptors increases with doping concentration. The interaction between the acceptors increases as they become closer, enhancing the attractive potential felt by the exciton. When comparing the BE binding energy dependence on the acceptor doping concentration [Figs. 4(a) and 4(b)], the more localized BE#2 is found to have a strong dependence on the acceptor concentration. The potential felt by BE#2 is due to the interacting acceptors and is modified when the average distance between the acceptors decreases due to the increase in doping concentration. The binding energy for BE#1 is not expected to change considerably. The small increase observed (≈ 1 meV) is believed to be due a weak interaction with more distant acceptors. It should be reminded that the Bohr radius of the Be acceptor (a_{Be}) and the FE (a_{FE}) in GaAs is approximately 20 and 115 Å, respectively. At a doping concentration of 3×10^{17} cm^{-3}, it can be assumed that $\bar{d}_I > a_{FE}$. BE#2 can be described as a single BE perturbed by the potential of close acceptors. BE#1, on the other hand, has

basically the same origin, except that BE#1 is just slightly perturbed by distant neighbors [Fig. 4(b)].

The exciton decay time $\tau = 660$, 560, and 200 ps for BE#2 (a), BE#1 (b), and FE (c), respectively, is a consequence of the kinetic interplay between the three excitonic levels. At low temperatures, a FE can either decay radiatively or become trapped by the acceptor(s) to form a BE. This fact results in a smaller measured decay time for the FE in comparison with an undoped QW without a competing BE channel. BE#1 can similarly either decay radiatively or be trapped at interacting acceptors. BE#2, on the other hand, can only decay radiatively at the lowest temperatures assuming that nonradiative channels are negligible. Based on these arguments, we conclude that the difference between the PL and PLE spectra (the doublet structure is not observed in PLE) reflects the fact that the optical absorption is proportional to the density of state and is not influenced by excitation transfer.

The intensity ratio BE#2 versus BE#1 in the PL spectra depends strongly on the laser excitation power, also a consequence of the kinetic interplay situation between the three exciton levels. Low excitation power and temperature favor BE#2, seen experimentally, as a relatively high PL intensity. At these conditions, a large fraction of the excitons is trapped by the interacting acceptors. An increase in the excitation power is followed by an increase in the intensity of the single acceptor BE (BE#1) relative to BE#2, since a saturation effect of excitons bound at interacting acceptors is achieved.

The magnetic field dependence of BE#2 can be explained in terms of the shrinking of the wave functions (decrease in the Bohr radius) of the exciton. For an exciton that interacts with, e.g., a pair of acceptors separated by a certain distance d_I, the effect of a magnetic field is to shrink their wave function until the exciton interacts only with one of the acceptors (resulting in a BE#1) or has just a weak interaction with the second acceptor.

The temperature dependence of the FE and BE intensities is well known in the literature.[9] The region $T_a < T < T_b$, seen in the inset of Fig. 6, corresponds to a temperature range where the capture rate of excitons by the acceptors increases. The increase of the capture rate is due to the thermal activation of the FE localized at interface roughness potentials, resulting in an increase of the mean thermal velocity of the FE.[10]

The temperature behavior of the BE's at $T_a < T < T_b$ has similarities with the laser intensity dependence, as discussed above. We propose that the exponential decay of the BE#2 intensity followed by an increase in the BE#1 can be understood as a continuous thermal activation of the BE#2 state into the BE#1 state. The BE#2 is continuously delocalized from the interacting acceptors potential to a higher state, i.e., BE#1, as they gain thermal energy ($k_B T$). Following the same arguments, BE#1 will dissociate into FE's for temperatures above T_b. This is seen in Fig. 6 as a decrease of the intensity of BE#1 parallel with an increase of the FE intensity. Finally, at T_c, the BE's are quenched and also the FE population starts to dissociate. The temperatures T_b and T_c are accordingly correlated to temperatures for the dissociation of BE#1's and FE's, respectively.

V. SUMMARY

In summary, we have studied the effect of an increasing acceptor concentration (between 10^{16} and 10^{18} cm^{-3}) on acceptor-bound excitons. Low excitation power and temperature favor an exciton bound at interacting acceptors. An increase in the excitation power is followed by an increase in the intensity of the ''normal'' single acceptor BE (BE#1), since more excitons are available due to saturation effects of the interacting acceptor BE. The BE#2 intensity decreases continuously with temperature and quenches at approximately 45 K due to the small difference in binding energy compared to BE#1. The BE#2's are also very sensitive to the applied magnetic field. The intensity decrease with increasing magnetic field can be explained in terms of the shrinking of the wave functions (decreasing of the Bohr radius) of the BE#2's. For an exciton interacting with, e.g., a pair of acceptors separated by a certain distance, the magnetic field will give rise to a shrinkage of the wave function until the exciton interacts only with one of the acceptors.

ACKNOWLEDGMENT

[1] J. J. Hopfield, H. Kukimoto, and P. J. Dean, Phys. Rev. Lett. **27**, 139 (1971); T. N. Morgan, M. R. Lorenz, and A. Onton, *ibid.* **28**, 906 (1972).

[2] R. A. Street and P. J. Wiesner, Phys. Rev. Lett. **34**, 1569 (1975); Phys. Rev. B **14**, 632 (1976); P. J. Wiesner, R. A. Street, and H. D. Wolf, Phys. Rev. Lett. **35**, 1366 (1975).

[3] A. C. Ferreira, P. O. Holtz, B. E. Sernelius, A. Buyanov, B. Monemar, O. Mauritz, U. Ekenberg, M. Sundaram, K. Campman, J. L. Merz, and A. C. Gossard (unpublished).

[4] S. J. Pearton, Int. J. Mod. Phys. B **8**, 1244 (1994).

[5] I. Buyanova, A. C. Ferreira, P. O. Holtz, B. Monemar, K. Campman, J. L. Merz, and A. C. Gossard, Appl. Phys. Lett. **68**, 1365 (1996).

[6] P. J. Dean and A. M. White, Solid State Electron. **21**, 1351 (1978).

[7] B. Monemar, N. Magnea, and P. O. Holtz, Phys. Rev. B **33**, 7375 (1986).

[8] E. Molva and N. Magnea, Phys. Status Solidi **102**, 475 (1980).

[9] See, for example, J. P. Bergman, P. O. Holtz, B. Monemar, M. Sundaram, J. L. Merz, and A. C. Gossard, in *Impurities, Defects and Diffusion in Semiconductors: Bulk and Layered Structures*, edited by D. J. Wolford, J. Bernholc, and E. E. Haller, MRS Symposia Proceedings No. 163 (Materials Research Society, Pittsburgh, 1990).

[10] C. I. Harris, B. Monemar, P. O. Holtz, H. Kalt, M. Sundaram, J. L. Merz, and A. C. Gossard (unpublished).